1.E1; 2.E

Nuclear Physics **45** (1963) 273—295; © *North-Holland Publishing Co., Amsterdam*

THE ^{23}Na(d, p)^{24}Na REACTION AND THE NUCLEAR STRUCTURE OF ^{24}Na

C. DAUM †

Harrison M. Randall Laboratory of Physics, University of Michigan, Ann Arbor, Michigan

Received 20 February 1963

Abstract: The level scheme of ^{24}Na up to about 7 MeV has been studied with the ^{23}Na(d, p)^{24}Na reaction. Several new levels have been observed. A few discrepancies in energy assignment to levels exist between these and earlier experiments. The angular distributions have been analysed with the DWBA analysis. A BBA analysis checks well with earlier results. Spectroscopic data have been obtained for many of the levels. A discussion of the nuclear structure of ^{24}Na will follow in a second paper [28]).

1. Introduction

The nucleus ^{24}Na has been studied as part of a group of investigations of the nuclei in the (1d-2s) shell at the cyclotron laboratory of the University of Michigan. This particular nucleus is an interesting case, since it is an odd nucleus in which the coupling of the odd proton and the odd neutron causes complications in the interpretation of the structure.

The investigation has been carried out with the help of the ^{23}Na(d, p)^{24}Na reaction by making use of the external beam of 7.8 MeV deuterons produced by the cyclotron. The protons were detected with nuclear emulsion plates in the image plane of a magnetic spectrometer.

2. The (d, p) Reaction. Direct Reaction Theory

Currently the angular distributions of the (d, p) reaction are analysed with the Butler Born Approximation (BBA)[1, 2]) and the Distorted Wave Born Approximation (DWBA)[3, 4]). The BBA analysis leads to spectroscopic information in terms of a quantity

$$(T_i \tfrac{1}{2} T_{zi} \tfrac{1}{2} | T_f T_{zf})^2 (2J_f + 1)\theta_i^2 = (T_i \tfrac{1}{2} T_{zi} \tfrac{1}{2} | T_f T_{zf})^2 (2J_f + 1) S_l \theta_0^2(nl), \qquad (1)$$

for each transition. Here, J_f is the spin of the state of the final nucleus, θ_i^2 is the reduced width of the (d, p) transition to this state, S_l is the spectroscopic factor, which corresponds to an angular momentum transfer $\hbar l$ by the captured neutron, $\theta_0^2(nl)$ is the single particle reduced width for the capture of the transferred neutron

† On leave of absence from and now at the Instituut voor Kernphysisch Onderzoek, Amsterdam, The Netherlands.

into a single particle state $|nl\rangle$. The Clebsch-Gordan coefficient represents the coupling of the isobaric spin of the initial nucleus to that of the neutron resulting in the isobaric spin of the final nucleus.

The DWBA analysis calculates the differential cross section $\sigma(\theta)_{nl,\,\text{single particle}}$ for a single particle transition to a state $|nl\rangle$ in zero-range approximation for an exponential wave function of the deuteron. Hence

$$\sigma_l(\theta) = (T_i \tfrac{1}{2} T_{zi} \tfrac{1}{2} | T_f T_{zf})^2 \frac{2J_f+1}{2J_i+1} S_l \sigma(\theta)_{nl,\,\text{single particle}}. \tag{2}$$

Here, J_i is the spin of the target nucleus, $\sigma_l(\theta)$ is the experimental differential cross section, all other symbols have been defined before. Instead of using an exponential wave function for the deuteron, it may be more appropriate to use the Hulthén wave function. Then

$$\sigma_l(\theta)(\text{zero range}) = (T_i \tfrac{1}{2} T_{zi} \tfrac{1}{2} | T_f T_{zf})^2 \frac{2J_f+1}{2J_i+1} S_l \, 1.48 \sigma(\theta)_{nl,\,\text{single particle}}. \tag{3}$$

A correction for finite range effects can be considered. However, the correction can only be estimated for incident and outgoing plane waves. We obtain

$$\sigma_l(\theta)(\text{finite range}) = \left(\frac{\beta^2}{K^2+\beta^2}\right)^2 \sigma_l(\theta)(\text{zero range}). \tag{4}$$

Here, β is the inverse of the range of the short range term in the Hulthén wave function and $\hbar K$ is the internal momentum of the deuteron. This correction is a lower limit on the correction in the distorted wave theory.

With the help of these formulae we obtain from the experiment the ratio between the experimental and theoretical value of the differential cross section in the first maximum of the angular distribution. This ratio is

$$1.48 \left(\frac{\beta^2}{K^2+\beta^2}\right)^2 (T_i \tfrac{1}{2} T_{zi} \tfrac{1}{2} | T_f T_{zf})^2 \frac{2J_f+1}{2J_i+1} S_l. \tag{5}$$

We propose to call $(T_i \frac{1}{2} T_{zi} \frac{1}{2} | T_f T_{zf})^2((2J_f+1)/(2J_i+1))S_l$ the spectroscopic ratio. The ratio (5) contains all spectroscopic information, except for the factor 1.48 $(\beta^2/(K^2+\beta^2))^2$, which is due to the description of the reaction mechanism.

The advantage of the DWBA above the BBA is that a fit may be obtained to the angular distributions and that mixtures of l components may be separated in a more reliable way than with the BBA.

3. Experimental Arrangement

The instrumentation for nuclear spectroscopy at the University of Michigan has been described in extenso by Bach, Childs, Hockney, Hough and Parkinson [5]). An energy resolution of about 20 keV is obtained in the present experiment.

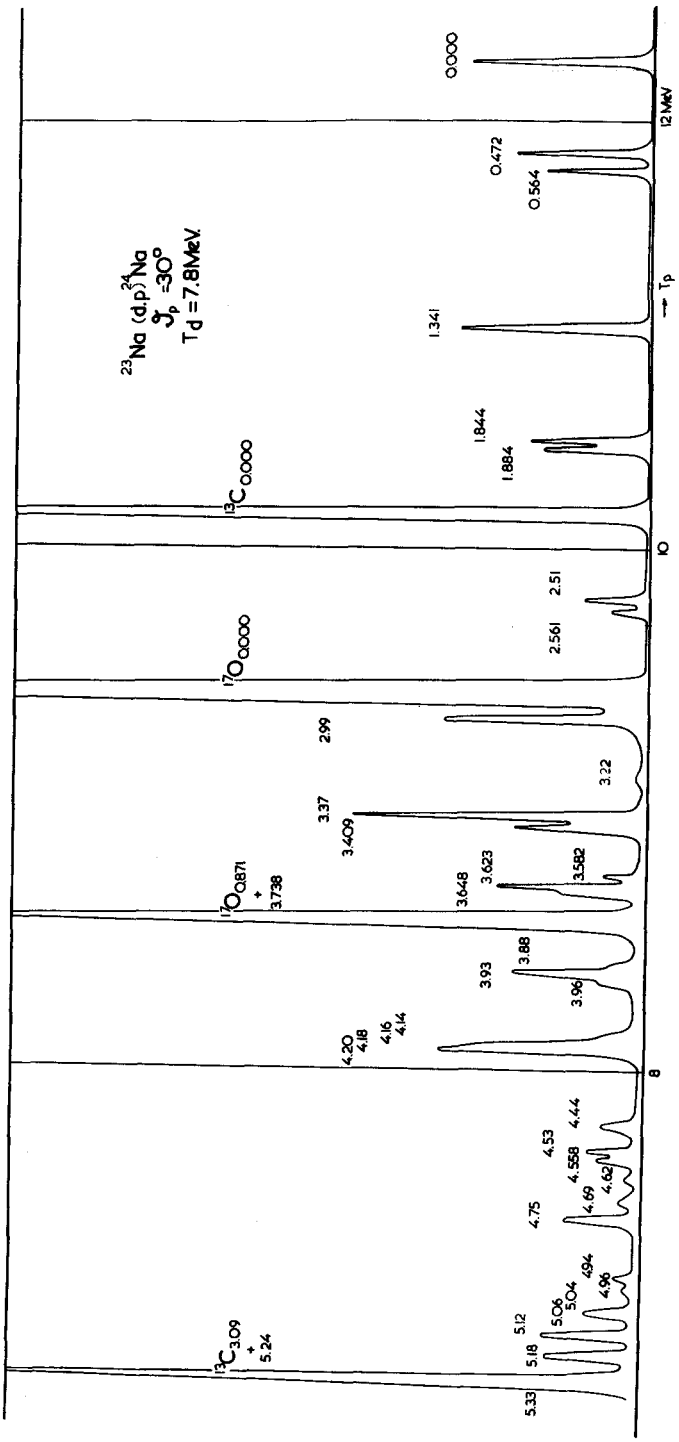

Fig. 1(a). Spectrum of the protons of the $^{23}Na(d, p)^{24}Na$ reaction at an angle of 30° with the incident beam. The vertical axis is the number of proton tracks in arbitrary units.

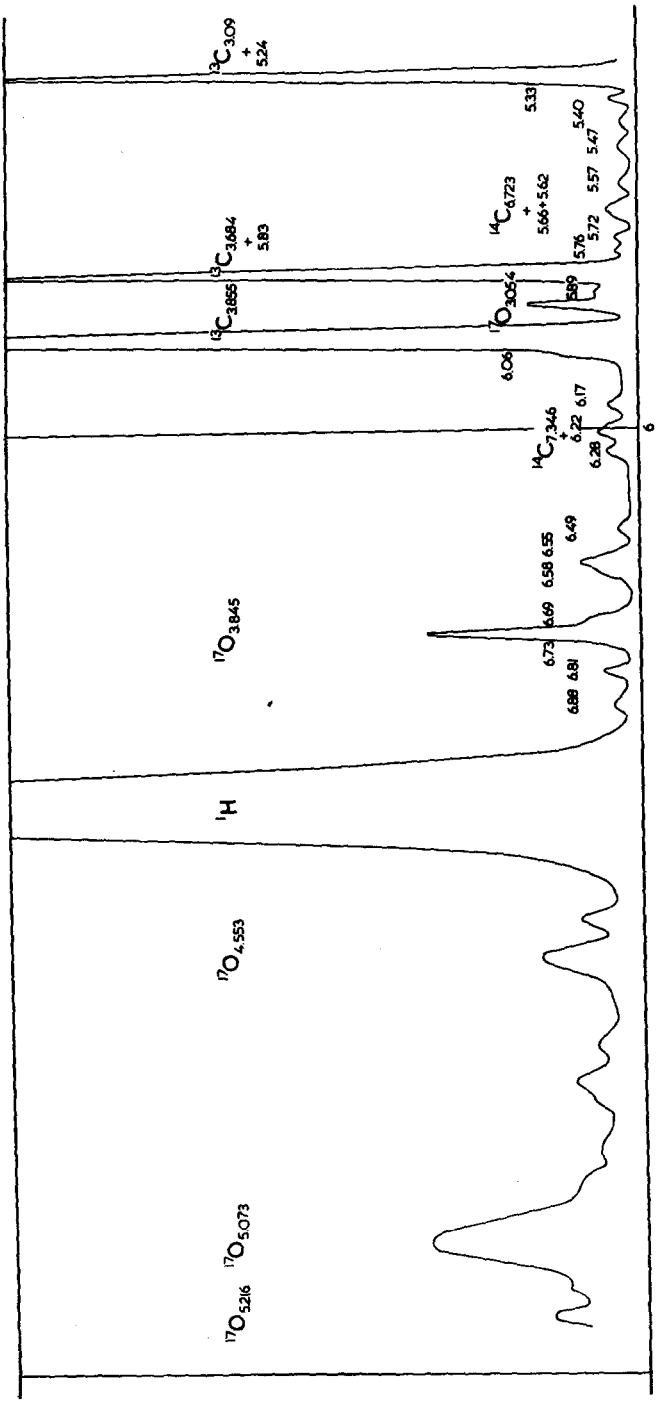
$^{13}C_{3.09}$ + 5.24
5.33
5.40
5.47
$^{14}C_{4.723}$ + 5.66+5.62
5.57
5.76
5.72
$^{13}C_{3.684}$ + 5.83
$^{13}C_{3.885}$
$^{17}O_{3.054}$
5.89
6.06
$^{14}C_{7.346}$ + 6.22
6.17
6.28
6
$^{17}O_{3.845}$
6.49
6.55
6.58
6.69
6.73
6.81
6.88
^{1}H
$^{17}O_{4.553}$
$^{17}O_{5.073}$
$^{17}O_{5.216}$
4

Fig. 1(b).

Targets have been made by evaporation of NaOH on a gold leaf backing of about 0.2 μg/cm^2. The amount of Na on various targets was between 8 and 140 μg/cm^2. The target thickness has been measured by neutron activation analysis with the help of the ^{23}Na(n, γ)^{24}Na reaction. The accuracy of the method was about $\pm$ 8 percent. This method has been proposed by Professor Meinke of the Nuclear Chemistry group at the Phoenix reactor of the University of Michigan. The measurements have been performed by Mr. H. M. Nass, research assistant of this group (see also ref.[6]) for this method).

4. The Experimental Results

In the present investigation angular distributions of protons from the ^{23}Na(d, p) ^{24}Na reaction have been obtained at angles from 10° to 50° in steps of 5° and at larger angles up to 90° in steps of 10°. Points of the angular distribution at 0° and 5° have been measured for transitions to levels in the first 3.5 MeV excitation of ^{24}Na, if these transitions show up strongly at these angles.

Fig. 1 shows a typical spectrum at a laboratory angle of 30°. The figure shows a large number of well separated peaks of protons from the stripping reaction leaving ^{24}Na in excited states. Evidently, the good resolution of the proton peaks makes possible the assignment of spectroscopic labels to many states of ^{24}Na. In addition, several new peaks have been found in the region of excitation of ^{24}Na up to 5.5 MeV and new levels have been identified in the region from 5.5-7 MeV excitation. Several peaks are found, which are due to the contamination of C, O and H in the target. Unfortunately, in the region of excitation of ^{24}Na above 5 MeV these peaks coincide with peaks of the ^{23}Na(d, p)^{24}Na reaction at several angles. Therefore, parts of the angular distributions to levels of ^{24}Na in this region cannot be obtained.

Figs. 2a, b, c and d show the plots of the angular distributions for the elastic scattering of deuterons on ^{23}Na and for the (d, p) transitions to levels of ^{24}Na. The curves through the experimental points are DWBA fits to the angular distributions. These fits will be discussed in sect. 6.

5. The Errors

The error in the Q value of a transition, hence the error in the excitation energy E_x of a level of ^{24}Na, is of the order of the resolution, which has been obtained in the experiment. Then, a good estimate of the error in Q and E_x is $\pm$ 20 keV.

The error bars on the experimental points of the angular distributions have been calculated taking into account the effect of all sources of error (see ref. [7])). The errors represent the error in the relative position of the points. The error in the absolute scale is about $\pm$ 8 percent and it is due to the uncertainty of the measurement of the target thickness.

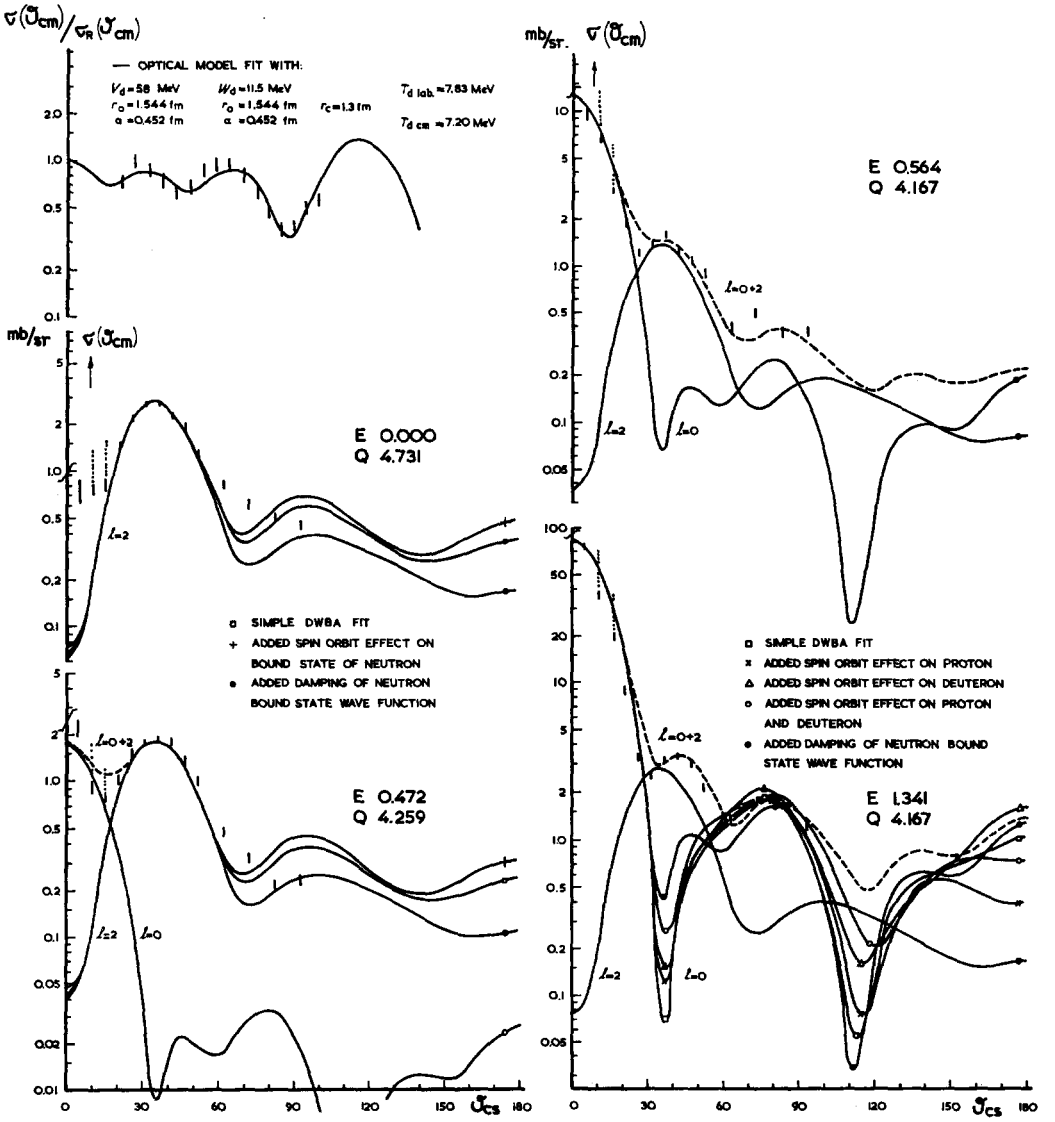
σ(ϑcm)/σR(ϑcm)
— OPTICAL MODEL FIT WITH:
Vd = 58 MeV
Wd = 11.5 MeV
Td lab. = 7.83 MeV
r0 = 1.544 fm
r0 = 1.544 fm
rc = 1.3 fm
a = 0.452 fm
a = 0.452 fm
Td cm = 7.20 MeV
mb/sr
σ(ϑcm)
E 0.000
Q 4.731
L=2
□ SIMPLE DWBA FIT
+ ADDED SPIN ORBIT EFFECT ON BOUND STATE OF NEUTRON
• ADDED DAMPING OF NEUTRON BOUND STATE WAVE FUNCTION
L=0+2
E 0.472
Q 4.259
L=2
L=0
mb/sr.
σ(ϑcm)
E 0.564
Q 4.167
L=0+2
L=2
L=0
□ SIMPLE DWBA FIT
× ADDED SPIN ORBIT EFFECT ON PROTON
△ ADDED SPIN ORBIT EFFECT ON DEUTERON
○ ADDED SPIN ORBIT EFFECT ON PROTON AND DEUTERON
• ADDED DAMPING OF NEUTRON BOUND STATE WAVE FUNCTION
L=0+2
E 1.341
Q 4.167
L=2
L=0
0 30 60 90 120 150 ϑcs 180

Fig. 2(a).

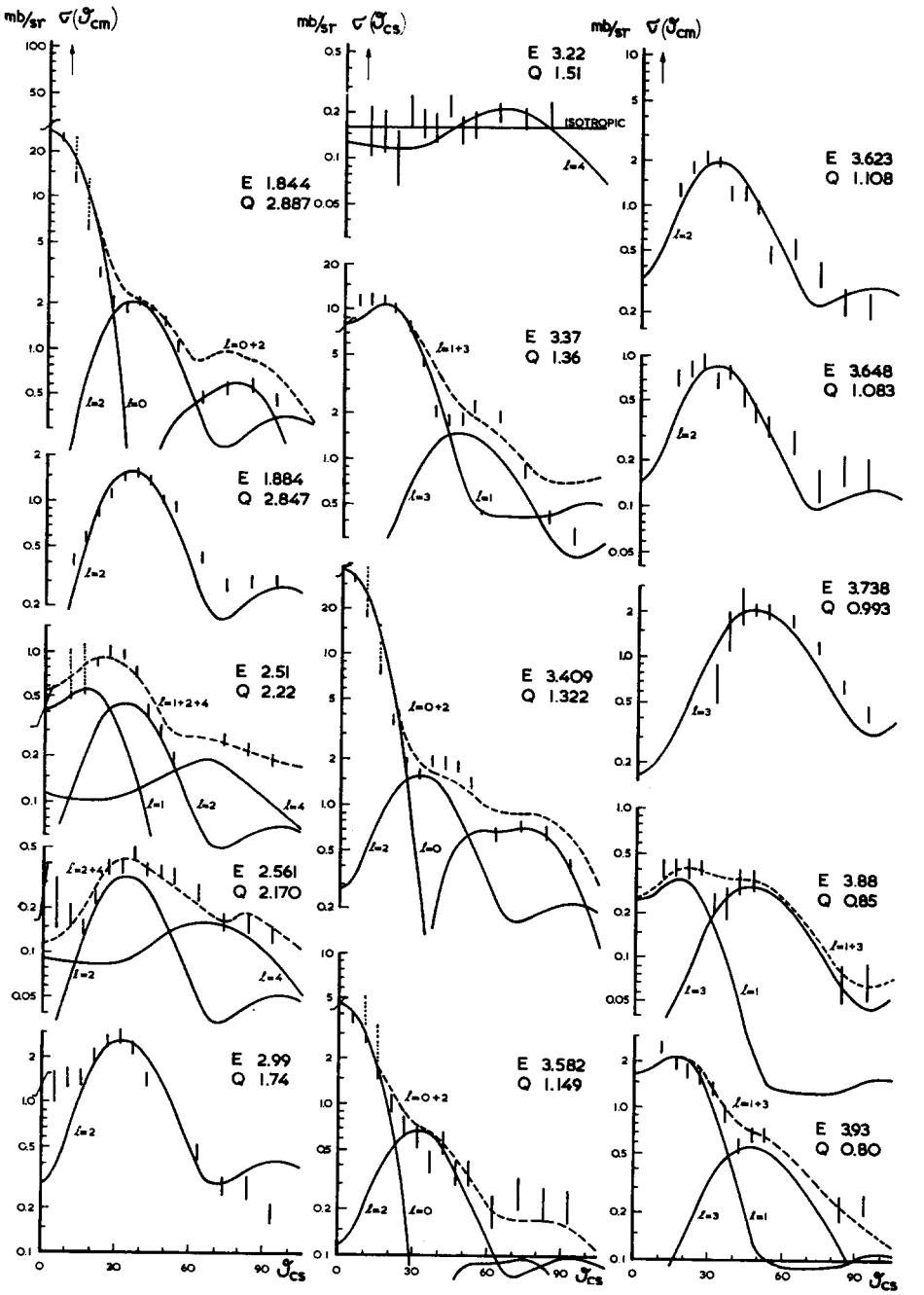
mb/sr σ(ϑcm)
mb/sr σ(ϑcs)
mb/sr σ(ϑcm)
E 1.844
Q 2.887
E 3.22
Q 1.51
ISOTROPIC
E 3.623
Q 1.108
E 3.37
Q 1.36
E 3.648
Q 1.083
E 1.884
Q 2.847
E 3.738
Q 0.993
E 2.51
Q 2.22
E 3.409
Q 1.322
E 3.88
Q 0.85
E 2.561
Q 2.170
E 2.99
Q 1.74
E 3.582
Q 1.149
E 3.93
Q 0.80
ϑcs

Fig. 2(b).

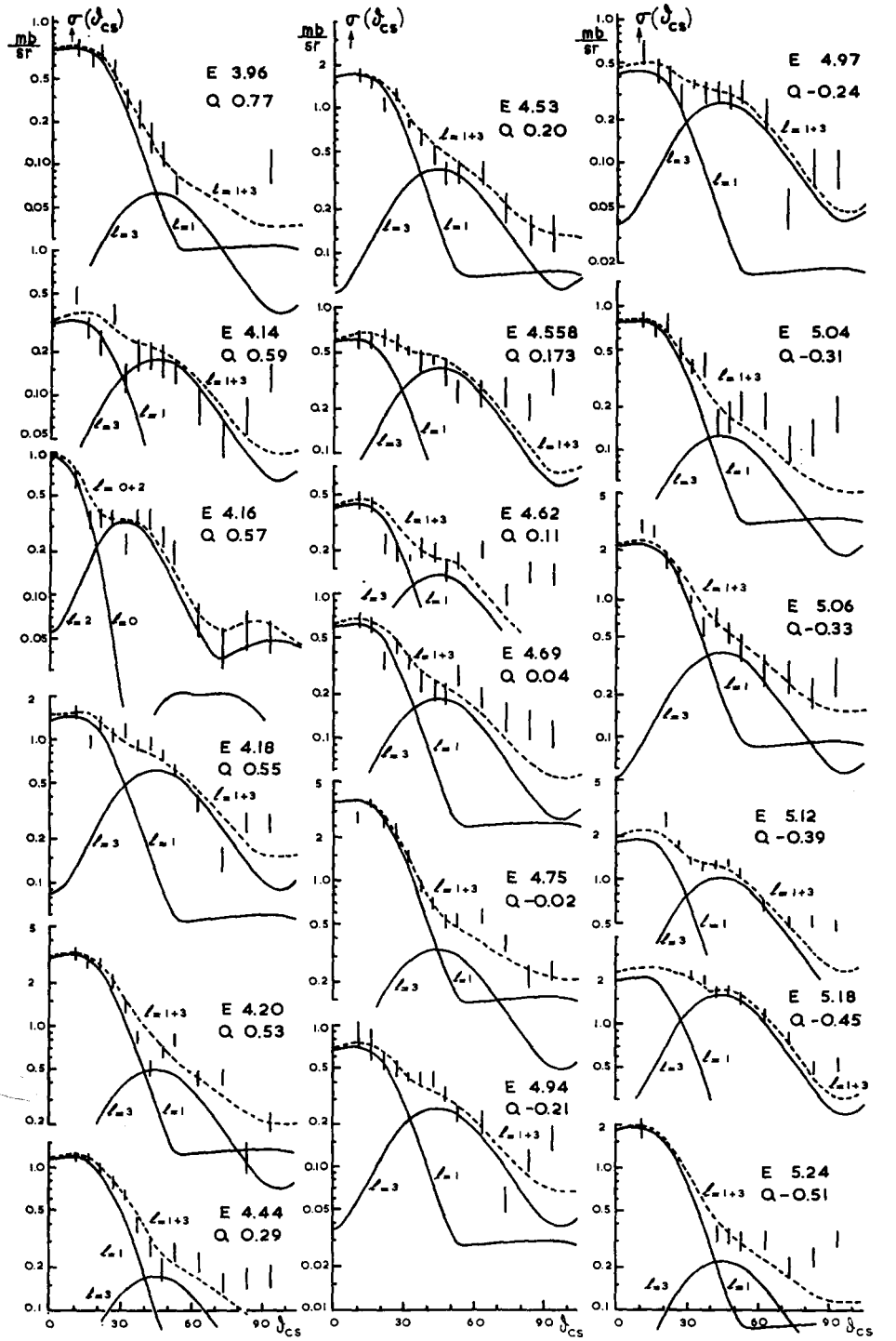
σ(ϑcs)
mb/sr
E 3.96
Q 0.77
E 4.14
Q 0.59
E 4.16
Q 0.57
E 4.18
Q 0.55
E 4.20
Q 0.53
E 4.44
Q 0.29
E 4.53
Q 0.20
E 4.558
Q 0.173
E 4.62
Q 0.11
E 4.69
Q 0.04
E 4.75
Q -0.02
E 4.94
Q -0.21
E 4.97
Q -0.24
E 5.04
Q -0.31
E 5.06
Q -0.33
E 5.12
Q -0.39
E 5.18
Q -0.45
E 5.24
Q -0.51
ϑcs

Fig. 2(c).

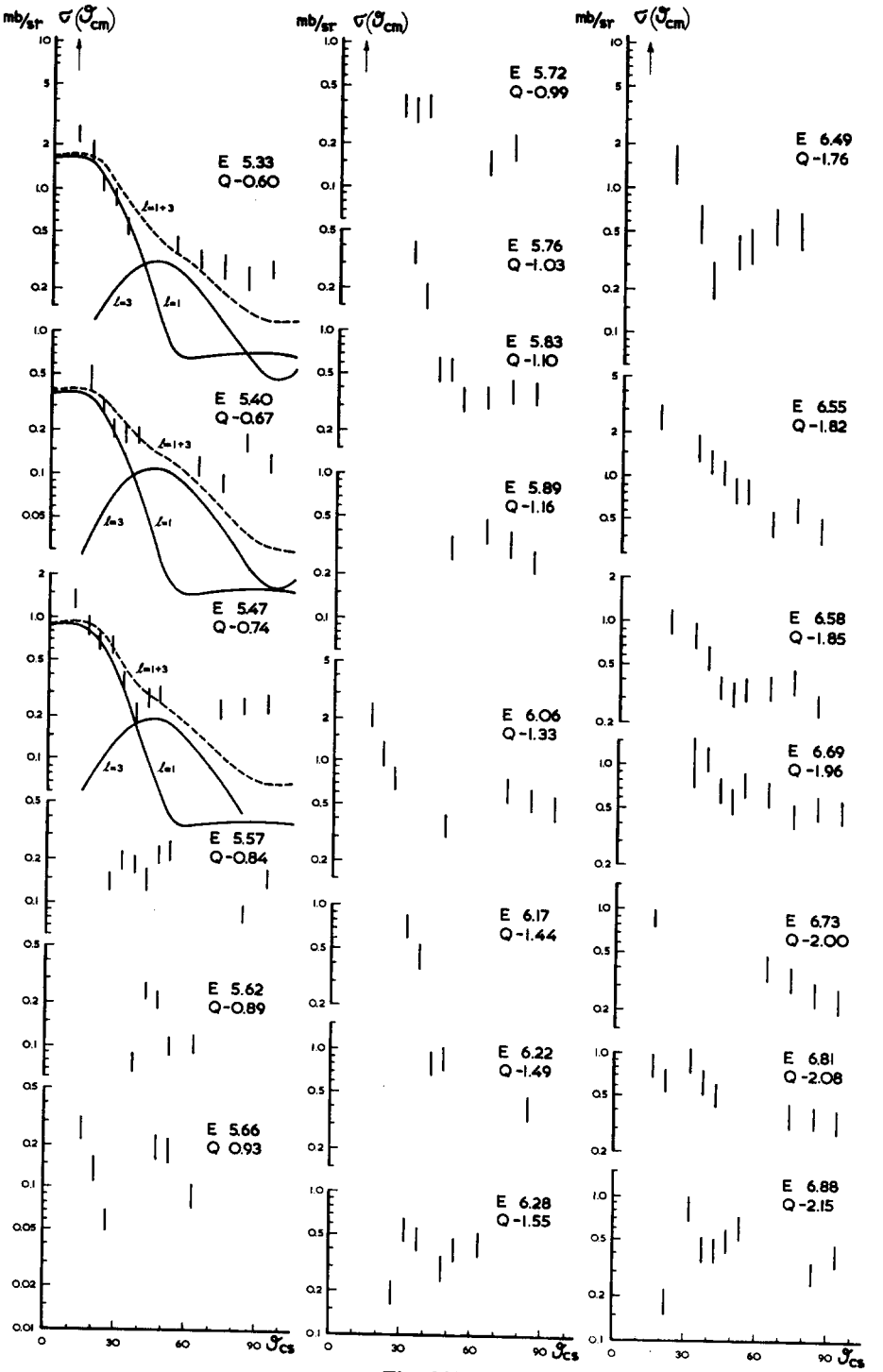
mb/sr σ(ϑcm)
E 5.33
Q -0.60
E 5.40
Q -0.67
E 5.47
Q -0.74
E 5.57
Q -0.84
E 5.62
Q -0.89
E 5.66
Q 0.93
E 5.72
Q -0.99
E 5.76
Q -1.03
E 5.83
Q -1.10
E 5.89
Q -1.16
E 6.06
Q -1.33
E 6.17
Q -1.44
E 6.22
Q -1.49
E 6.28
Q -1.55
E 6.49
Q -1.76
E 6.55
Q -1.82
E 6.58
Q -1.85
E 6.69
Q -1.96
E 6.73
Q -2.00
E 6.81
Q -2.08
E 6.88
Q -2.15
ϑcs

Fig. 2(d).

6. Analysis of the Angular Distributions

The spin and parity of the ground state of ^{23}Na is $\frac{3}{2}^+$. Therefore, levels of ^{24}Na with non-zero spin can be produced by several ways of angular momentum transfer in agreement with the selection rules [1]), i.e. the angular distributions of transitions contain more l components, combinations of l even or odd depending on the parity of the final state. We have pointed out in section 2, that the DWBA analysis may be successful in separating these l components.

The distorted waves in the DWBA analysis can be obtained from an optical model analysis of the elastic scattering of deuterons and protons on the considered nuclei. The optical model parameters of the incident deuteron wave are obtained from a "best" fit to the ^{23}Na(d, d)^{23}Na angular distribution. A ^{24}Na(p, p)^{24}Na experiment, for obtaining the parameters for the outgoing proton wave, is of course not possible. In such a case a choice of these parameters can be made by comparison with the (p, p) experiment on neighbouring nuclei under the assumption, that the parameters do not change appreciably over a small range of isotopes.

The calculations have been carried out by Satchler [3]). The "best" fit to the ^{23}Na (d, d)^{23}Na angular distribution (fig. 2a) is obtained with a real Woods-Saxon potential $V(r) = -V/[\exp((r-r_0A^{\frac{1}{3}})/a)+1]$, where $V = 58$ MeV, $r_0 = 1.544$ fm and $a = 0.452$ fm, an imaginary Woods-Saxon potential, where $W = 11.5$ MeV, $r_0 = 1.544$ fm and $a = 0.452$ fm (replace V in the real potential by W), and a Coulomb potential, which is the potential of a uniformly charged sphere of radius $r_cA^{\frac{1}{3}} = 1.3\ A^{\frac{1}{3}}$ fm, and charge $Z = 11$.

Fig. 2a, b, c, d. Angular distributions of the ^{23}Na(d, d)^{23}Na and the ^{23}Na(d, p)^{24}Na reaction at a deuteron energy of 7.8 MeV. The vertical axis is the ratio of the experimental differential cross section and the Rutherford cross section for the elastic scattering and the differential cross section for the (d, p) reaction in mb/sr. The horizontal axis represents the angle in the centre-of-mass system. The error bars have been obtained from an error calculation for the relative position of the points. The error in the absolute scale is about 8 %. The dotted extension on the error bars at 10° and 15° is a possible extra uncertainty due to misalignment of the spectrometer. E is the excitation energy of the level and Q the Q value of the (d, p) reaction to the level, both in MeV.

DWBA: the optical model parameters, presented in fig. 2a, of the deuteron wave are obtained from the (d, d) curve. These parameters provide the "best" fit, represented by the solid line, to the experimental points.

The chosen optical model parameters of the proton wave are: $V(r) = -V/(\exp((r-r_0A^{\frac{1}{3}})/a)+1)$, $V = 53$ MeV, $r_0 = 1.25$ fm, $a = 0.65$ fm, $W(r) = W(\mathrm{d}/\mathrm{d}x)(1/(\exp x+1))$, $x = r-r_0A^{\frac{1}{3}}$, $W = 46$ MeV, $r_0 = 1.25$ fm, $a = 0.47$ fm, Coulomb potential: uniformly charged sphere of radius $r_0A^{\frac{1}{3}} = 1.25A^{\frac{1}{3}}$ fm.

In fig. 2a, □ denotes the simple DWBA fit; + added spin-orbit coupling of 30× the Thomas spin-orbit coupling and a neutron bound state wave function in a Woods-Saxon well of radius $1.25\ A^{\frac{1}{3}}$ fm and surface thickness 0.65 fm for a binding energy $Q+2.226$ MeV; ● added damping of the neutron bound state wave function by $\exp(-((r-R_n)/A_n)^2)$ for $r < R_n = 5$ fm, $A_n = 3$ fm; × added spin-orbit coupling on proton, $V_{so} = 8$ MeV; △ added spin-orbit coupling on deuteron, $V_{so} = 10$ MeV; ○ added spin-orbit coupling on proton and deuteron. In figures 2b, c, d only the fit □ has been applied.

The solid lines are the DWBA curves for the l values shown on the curves, the dashed lines are the fits to the experimental points by summing DWBA curves for several l values.

As can be seen from fig. 2a the fit is not particularly good. The remaining discrepancies may just reflect imperfect averaging of the compound nucleus effects, i.e. the optical model may only give an average description at this energy. For example, there is some evidence for this effect from measurements by Mayer-Böricke, Santo and Schmidt-Rohr [8]) of Mg(d, d)Mg distributions in an energy range of deuterons of 8-12 MeV. These data show slight fluctuations of the order of the discrepancy between the present experiment and the DWBA fit (Satchler).

The parameters, chosen to describe the outgoing proton wave, are a real Woods-Saxon potential with $V = 53$ MeV, $r_0 = r_c = 1.25$ fm and $a = 0.65$ fm and for the imaginary part a surface absorption potential $W(r) = +W(\mathrm{d}/\mathrm{d}x)(1/(\exp x+1))$ where $x = (r-r_0'A^{\frac{1}{3}})/a'$, with $W = 46$ MeV, $r_0' = 1.25$ fm and $a' = 0.47$ fm. The experience is that the calculated (d, p) angular distributions are very sensitive to the parameters of the deuteron wave, but depend less on those of the proton wave [3]).

Fig. 2a shows several DWBA fits to the transitions to the levels at 0.000, 0.472, 0.564 and 1.341 MeV. The simple DWBA fit [3]) is obtained with these optical model parameters and with a three-dimensional harmonic oscillator wave function for the bound state of the neutron. The differential cross section is obtained in zero-range approximation.

The simple DWBA fit is extended by making the following additions:

(1) Spin-orbit effects on proton and deuteron are introduced using a Thomas type spin-orbit coupling of the form $-2V_{so}(1/r)(\mathrm{d}/\mathrm{d}r)((1/\exp((r-r_0A^{\frac{1}{3}})/a)+1))$ $\boldsymbol{l}\cdot\boldsymbol{s}$, where r_0 and a as for the real potential well and $V_{so} = 8$ MeV for protons and $V_{so} = 10$ MeV for deuterons. The value of V_{so} for deuterons is a reasonable guess, based on neutron and proton values.

The effect of the spin-orbit term is only appreciable in the backward direction, where no experimental points have been obtained. In particular, the deuteron spin-orbit coupling shows more influence on the cross section than the proton spin-orbit coupling. No experimental information is available about the magnitude of the deuteron spin-orbit coupling.

(2) The neutron bound state wave function is computed in a Woods-Saxon potential of radius $1.25\,A^{\frac{1}{3}}$ fm, surface thickness 0.65 fm, for a binding energy $Q+2.226$ MeV and for a spin-orbit coupling of 30 times the Thomas spin-orbit coupling. Comparison with the simple DWBA fit shows, that the effect of the change of the bound state wave function is small.

(3) The effect of the finite range of the V_{np} potential is estimated. It has been suggested that this effect would reduce contributions from the nuclear interior. To judge this effect (if real) in a rough way, the neutron wave function is multiplied by $\exp[-((r-R_n)/A_n)^2]$ for $r < R_n$, thus damping out interior contributions ($R_n = 5.0$ fm, $A_n = 3.0$ fm).

It is difficult to decide which case fits the experimental angular distributions best. It is worth noting that the forward spike of the $l = 2$ curve of the transition to the

ground state of ^{24}Na has not been reproduced. In the transition to the ground state of ^{24}Na an $l = 0$ admixture, to explain the forward spike, is not possible on the basis of the selection rules ($\frac{3}{2}^+$ to 4^+).

Scott [9]) has made a fit to this transition at a deuteron energy of 8.9 MeV including the forward spike. This author derives the optical model parameters from values used in the case of neighbouring nuclei by variation of these parameters within reasonable limits, until a satisfactory fit to the (d, p) transition to the ground state of ^{24}Na is obtained. However, the author does not check whether these parameters fit elastic scattering data of deuterons on ^{23}Na at a deuteron energy of 8.9 MeV. Miller [10]) has shown in the case of ^{206}Pb(d, p)^{207}Pb, that the optical model parameters that are able to reproduce the (d, p) data do not necessarily fit the elastic scattering of deuterons on ^{206}Pb, and that parameters able to reproduce the (d, d) data do not fit the stripping data.

Satchler has calculated (d, p) curves for ^{23}Na(d, p)^{24}Na, before the present data of the elastic scattering were available, by making use of the information about the optical model parameters for the deuteron wave, which describe the elastic scattering on neighbouring nuclei at deuteron energies around 10 MeV. The $l = 2$ (d, p) curves, calculated with these parameters, show a forward spike. However, the (d, d) curve, calculated with these parameters, does not fit the present elastic data very well. Also, the absolute magnitude of the single particle cross section seems to be too small.

This discrepancy may be due to the distortion of the internal wave function of the deuteron in the neighbourhood of the nucleus. The optical model calculations are adjusted implicitly to this distortion. However, the influence of the distortion may be different in the case of the elastic scattering and the stripping reaction. Therefore, the implicit adjustment in the optical model calculation of a fit to the angular distribution of the elastic scattering and a fit to the stripping angular distributions may lead to different optical model parameters for the deuteron wave.

In the transition to the ground state of ^{24}Na an $l = 4$ admixture may be possible, if one compares the angular distribution of the transition to the 0.000 MeV and 0.472 MeV level. The latter falls off more steeply towards large angles than the first. In the transition to the 0.472 MeV level an admixture of an $l = 0$ component is possible ($\frac{3}{2}^+$ to 1^+). In fig. 2a the theoretical $l = 0$ curve has been adjusted at 0° to a lower value of the cross section than the experimental point to account empirically in the $l = 2$ curve for the apparent forward spike, the magnitude of which has been estimated from the transition to the ground state.

Fig. 2a shows that the DWBA fits with the damped bound state wave function of the neutron may give the best fit to the transitions to the levels at 0.564 MeV and 1.341 MeV for an appropriate linear combination of the $l = 0$ and $l = 2$ components,

$$\sigma(\theta) = a_0\sigma(\theta)_{0\,\mathrm{th}} + a_2\sigma(\theta)_{2\,\mathrm{th}}. \tag{6}$$

It is evident from the formulae (2), (3) and (4), that $a_l = (T_i\tfrac{1}{2}T_{zi}\tfrac{1}{2}|T_fT_{zf})^2((2J_f+1)/(2J_i+1))S_l$, representing the spectroscopic ratio.

In the case of ^{23}Na(d, p)^{24}Na, $T_i = \frac{1}{2}$, $T_{zi} = \frac{1}{2}$, $T_f = 1$, $T_{zf} = 1$, and the Clebsch-Gordan coefficient is equal to unity. Hence

$$a_l = \left((2J_f+1)/(2J_i+1)\right) S_l. \tag{7}$$

It is evident that the a_l have to satisfy the condition

$$\sum_l a_l \leqq 1, \tag{8}$$

for a particular transition to a non-degenerate level, because a neutron cannot be captured in more than one single particle state. It is most likely that the levels of an odd nucleus like ^{24}Na are all non-degenerate, because the coupling of the odd nucleons would cause a cancellation of degeneracies.

Table 1 presents the DWBA analysis of the present experiment for the transitions to the ground state and the three lowest excited states of ^{24}Na, shown in fig. 2a.

The table shows that the relative spread in the values of the spectroscopic ratio, obtained for the various sets of optical model parameters which have been used in fig. 2a, amounts to about ± 15 percent. The error in the experimental value of the

TABLE 1

DWBA analysis of the (d, p) transitions to the levels in ^{24}Na at 0, 0.47, 0.56 and 1.34 MeV, for the sets of optical model parameters, shown in fig. 2a.

Level			Simple DWBA fit [e]			DWBA, zero range (form. (3)) [c] with spin-orbit coupling, neutron bound state in Woods-Saxon well				
			zero range form. (2) [b]	zero range form. (3) [c]	finite range form. (4) [d]	spin-orbit coupling on neutron only		added spin-orbit coupling on		
E_x(MeV)	J^{π} [a]	1)	a_l	a_l	a_l	a_l	damped bound state of neutron a_l	proton a_l	deuteron a_l	proton and deuteron a_l
0	4+	2	1.02	0.69	0.81	0.80	0.74			
0.47	1+	0	{0.02}	{0.014}	{0.014}	—	{0.02}			
		2	0.58	0.39	0.46	0.49	0.43			
0.56	(2)+	0	0.15	0.10	0.10	0.10	0.12			
		2	{0.45}	{0.30}	{0.35}	—	{0.32}			
1.34	1+	0	0.91	0.62	0.62	0.62	0.77	0.74	0.69	0.70
		2	{0.82}	{0.37}	{0.55}	—	{0.55}	—	—	—

Here is $a_l = ((2J_f+1)/(2J_i+1))S_l$, the spectroscopic ratio for an angular momentum transfer l.
The energy of the incident deuterons is 7.8 MeV.

[a]) for the discussion of J^{π}, see ref. [11]).

[b]) exponential wave function of the deuteron.

[c]) Hulthén wave function of the deuteron.

[d]) Hulthén wave function of the deuteron and finite range correction for a theory with incident and outgoing plane waves.

[e]) The bound state wave function of the neutron, is calculated in a harmonic oscillator well.

{ } means, values are to be doubted (see sect. 6).

TABLE 2

Comparison of BBA analyses by several authors and the present work for the (d, p) transitions to the first four levels of ^{24}Na

Level[a]	Level[b]		r_{co} = 5.65 fm		Level[c]				Level[d]	r_{co} = 5.64 fm	Level[e]	r_{co} = 5.17 fm		Level[f]	r_{co} = 5 fm			
E_x(MeV)	E_x(MeV)	J^π	l	θ^2_{rel}	E_x(MeV)	l	r_{co}	θ^2_{abs}	E_x(MeV)	l	E_x(MeV)	l	θ^2_{rel}	E_x(MeV)	l	θ^2_{rel}	θ^2_{abs}	θ^2_0(1d)[g]
0.000	0	4+	2	1	0	2	6	0.039	0	2	0	2	1	0	2	1	0.017	0.055
0.472	0.47	1+	2	3.9	0.47				0.47	2	0.48	2	1.5	0.47	2	2	0.035	0.067
			+															θ^2_0(1s)
0.564	0.56	(2)+	0	0.35	0.56				0.56	0	0.58	0	0.4	0.56	0	0.4	0.007	0.085
1.341	1.34	1+	0	2.5	1.34	0	6.2		1.34	0	1.34	0	4.6	1.34	0	4.8	0.082	0.098

[a]) T_d = 1.5-2.2 MeV, ref. [12])
[b]) T_d = 3 MeV ref. [13])
[c]) T_d = 14.8 MeV, ref. [14])
[d]) T_d = 8.6 MeV, ref. [15])
[e]) T_d = 8.9 MeV, ref. [16])
[f]) T_d = 7.8 MeV, present work.

[g]) the single particle reduced width, $\theta^2_0 = \theta^2_{abs}/S_l$, is obtained using the values of the spectroscopic ratio from table 1 for the zero range approximation with the Hulthén wave function.

differential cross section has been estimated to be of the order of 11 percent in these cases (see ref. [7])). Therefore, we may conclude that the experimental angular distributions in absolute units do not determine the exact form of the theory. It is also interesting to note that the sum rule (8) for the a_l is violated in the transition to the 1.341 MeV level, even in the case of the bound state wave function, which case gives a best fit to the experimental points in fig. 2a. Apparently, the theoretical $l = 0$ curves fall off to fast with increasing angle for angles larger than 15°. We may summarize that neither the shape of the angular distributions nor the absolute value of the differential cross section is conclusive for the exact form of the theory, and that reliable values of the absolute value of the spectroscopic ratio cannot be obtained in the present state of the theory. It is probably necessary to wait for good fits to (d, p) experiments on those neighbouring nuclei, which have an initial spin 0^+, in which case only one value l of angular momentum transfer is present in each transition.

Earlier (d, p) experiments on ^{23}Na by other authors have only been analysed with the BBA. Besides the DWBA fit, it is interesting to compare a BBA fit to the present experiment with the earlier data. Table 2 presents the results for the transitions to the first four levels of ^{24}Na. The single particle reduced widths $\theta_0^2(nl)$ in the last column are in fair agreement with those obtained in ref. [2]). The difference between $\theta^2_{abs} = 0.039$ ($\pm 30\%$) from Vogelsang's [14]) measurement and $\theta^2_{abs} = 0.017$ ($\pm 11\%$) from the present work for the transition to the ground state of ^{24}Na may be due to the energy dependence of θ_0^2(1d) or it may be due to the experimental errors.

We shall now proceed to the analysis of the transitions to the other levels of ^{24}Na. As a result of the above discussion we shall apply only the simple DWBA analysis in zero range approximation with a Hulthén deuteron wave function. Table 3 presents the value of $\sigma(\theta)_{nl,\text{ single particle}}$ (see form. (2)) for several values of l over a range of Q values.

TABLE 3

Absolute differential cross section in the first maximum of a single particle (d, p) transition in the DWBA analysis for ^{23}Na(d, p)^{24}Na

l	Q MeV	θ	$\sigma(\theta)_{nl,\text{ single particle}}$ (mb/sr)	Q MeV	θ	$\sigma(\theta)_{nl,\text{ single particle}}$ (mb/sr)
0	4.167	0°	90	0	0°	105
1	2.22	17°	22	0	12°	35
2	4.731	38°	2.85	0	29°	5.8
3	1.36	50°	1.2	0	42°	1.6
4	4.731	65°	0.54	0	58°	0.49

Table 4 presents the result of the DWBA analysis of all measured transitions. It also contains the energy assignments of the MIT group [12]) and the BBA analysis of the work by Dalton [16]). For purposes of comparison with the last work the results of the BBA analysis of the present experiments is included in the table.

TABLE 4

Levels of ^{24}Na. BBA and DWBA analysis of the ^{23}Na(d, p)^{24}Na reaction. Comparison with results of other authors.

Level [a])	Level [b])	BBA $r_{co} = 5.17$ fm		Level [c])	BBA $r_{co} = 5$ fm		DWBA 'zero range' including Hulthén normalizing factor (formula (3) [e]) Spectroscopic ratio: $((2J_t+1)/(2J_i+1))S_l$					
E_x(MeV)	E_x(MeV)	l	$(2J_t+1)\times\theta^2_{rel}$	[d]) E_x(MeV)	l	$(2J_t+1)\times\theta^2_{rel}$	$l=0$	$l=1$	$l=2$	$l=3$	$l=4$	J^π
0.000	0	2	9	0	2	9			0.69			4^+
0.472	0.48	2	4.6	0.47	2	6.1	(0.014)		0.39			1^+
0.564	0.58	0	2.0	0.56	0	2.0	0.10		(0.30)			$2^{+f})$
1.341	1.34	0	13.6	1.34	0	14.6	0.62		(0.37)			1^+
1.844	1.86	0	4.9	1.84	0	5.2	0.20		(0.39)			$1^+, 2^+$
1.884				1.88	2	4.3			0.29			$0^+, 1^+, 2^+, 3^+, 4^+$
2.464	2.52	2	7.9	2.51	1	—		(0.014)				$0^-, 1^-, 2^-, 3^-$
2.561				2.56	2	1.2			(0.08)		(0.26)	$0^{+g}), 1^{+g}), 2^+, 3^+, 4^+$
	2.95	—	—	2.99	2	5.7			0.068		(0.26)	$0^{+g}), 1^{+g}), 2^+, 3^+ 4^+$
				3.22	4	4.0			0.42			$0^+, 1^+, 2^+, 3^+, 4^+$
					or isotropic						(0.44)	$2^+, 3^+ 4^+, 5^+, 6^+$
				3.37	1	6.8		0.27		(0.85)		—
3.409	3.42	0 + 2	11.4 12.4	3.41	0	6.7	0.22		(0.24)			$2^-, 3^-$ $1^+, 2^+$
3.582	3.62	—	—	3.58	0	0.9	0.027		(0.09)			$1^+, 2^+$
3.623				3.62	2	4.6			0.27			$0^+, 1^+, 2^+, 3^+, 4^+$
3.648				3.65	2	2.1			0.13			$0^+, 1^+, 2^+, 3^+, 4^+$
3.738	—		—	3.74	3	1.5				1.03		$2^-, 3^-, 4^-, 5^-$
3.850	3.89	1	4.0	3.88	3	1.7		0.007		0.16		$2^-, 3^-$
3.899				3.93	1	1.3		0.051		0.29		$2^-, 3^-$
3.929				3.96	1	0.34		0.014		0.31		$2^-, 3^-$
				4.14	1	0.22		0.007		0.09		$2^-, 3^-$

4.184				4.16	0	0.18	0.007		(0.05)		1+, 2+
4.202	4.18	1	6.1	4.18	3	4.1		0.027		0.29	2−, 3−
4.219				4.20	1	1.5		0.068		0.24	2−, 3−
	4.41	1	0.93	4.44	1	0.53		0.027		0.074	2−, 3−
				4.53	1	0.78		0.034		0.17	2−, 3−
4.558	4.56	1	1.5	4.56	1	0.28		0.014		0.18	2−, 3−
				4.62	1	0.19		0.007		0.02	2−, 3−
				4.69	1	0.66		0.014		0.12	2−, 3−
	4.72	1	2.3	4.75	1	1.6		0.068		0.14	2−, 3−
	4.91	1	0.68	4.94	1	0.35		0.014		0.11	2−, 3−
				4.97	1	0.29		0.007		0.10	2−, 3−
	5.02	—	—	5.04	1	0.34		0.014		0.054	2−, 3−
				5.06	1	3.0		0.04		0.16	2−, 3−
	5.13	—	—	5.12	1	—		0.034		0.38	2−, 3−
				5.18	1	—		0.034		0.60	2−, 3−
				5.24	—	—		0.034		0.08	2−, 3−
	5.31	1	1.6	5.33	1	1.4		0.027		0.11	2−, 3−
	5.42	1	0.72	5.40	1	0.53		0.007		0.04	2−, 3−
				5.47	1	0.4		0.014		0.074	2−, 3−
				5.57	—	—					
				5.62	—	—					
				5.66	0[h])	—					
					+						1+, 2+
					2						

Other levels at 5.72, 5.76, 5.83, 5.89, 6.06, 6.17, 6.22, 6.28, 6.49, 6.55, 6.58, 6.69, 6.73, 6.81, 6.88 MeV.

[a]) T_d = 1.5-2.2 MeV, ref. [13]).
[b]) T_d = 8.9 MeV, ref. [16]).
[c]) T_d = 7.8 MeV, present work.
[d]) The error in E_x is ±0.02 MeV.
[e]) Since the finite range correction has not been applied, the spectroscopic ratios should be considered in relative units.
[f]) J^π is probably 2+ (see ref. [11]).
[g]) These values of J^π are excluded, if $l = 4$ is present.
[h]) The level at 5.66 MeV may have $l = 0$ and $l = 2$ and $J^\pi = 1^+$ or 2^+.
() means values are not reliable (see section [6])); we have not made a decision about the reliability of the spectroscopic ratios of the $l = 1$ and $l = 3$ components of the transitions to most of the odd parity levels.

Fig. 3 shows the distribution of the spectroscopic ratio for each value of l (from table 4) over the investigated region of excitation of ^{24}Na.

Table 4 shows three $l = 4$ transitions, which have a spectroscopic ratio unexpectedly high on the basis of any nuclear model. E.g. in the shell model the distance between the (1d-2s) shell and the (1g-2d-3s) shell is expected to be of the order of 10-15 MeV for ^{24}Na. It is difficult to construct any matrix element for an interaction which is strong enough to couple states of these two shells to contribute such strong $l = 4$ components to the present angular distributions. This may mean that the absolute

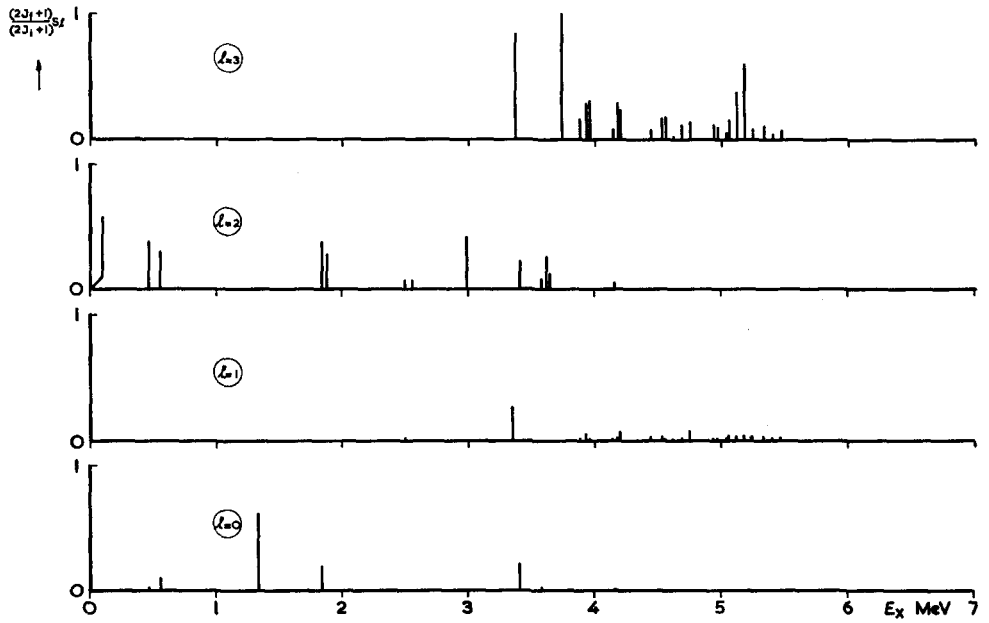

Fig. 3. The distribution of the values of the spectroscopic ratio $((2J_t+1)/(2J_i+1))S_l$ for each value of l as a function of the excitation energy E_x (from table 4).

magnitude of the theoretical $l = 4$ component is too small or that some other effect, not accounted for by the DWBA, is responsible for the high points around 60° in the experimental angular distributions. Also, the $l = 3$ components in the transitions to the 3.37 MeV and the 3.738 MeV levels seem to be large, indicating that the absolute magnitude of the DWBA fit for $l = 3$ is too small.

7. Discussion of the Levels of ^{24}Na

Fig. 24.1 of ref. [11]) shows the level diagram of ^{24}Na, from results before October 1961, including the preliminary results of the present work. In the present work many groups of levels of ^{24}Na have been resolved for the first time and spectroscopic information has been obtained for the individual levels. Some levels require a dis-

cussion in connection with earlier results. Sperduto and Buechner [12]) have reported levels at 2.464 and 2.561 MeV. In a later ^{31}P(d, p)^{32}P measurement, where the Na lines are present as contaminant, Piraino, Paris and Buechner [17]) confirm these states of ^{24}Na. However, these authors show a spectrum from which one may conclude that the two levels are more likely to be about 50 keV apart instead of 100 keV. We suppose that, in the first measurement of Sperduto and Buechner, confusion has occurred with a transition to a level in ^{28}Si. We conclude that the levels are at 2.51 MeV and 2.561 MeV.

The level at 2.51 MeV seems to be a doublet, consisting of an odd and an even parity level, which has not been resolved experimentally. Scott [9]) has already noted the strange shape of the combined angular distribution of the transition to the 2.51 MeV and the 2.561 MeV levels, which he has not resolved. He can fit the angular distribution with a DWBA calculation for $l = 2$ only, concluding that either both levels are due to $l = 2$ transitions or one predominantly so.

The present experiment shows that the difficulty is shifted to the transition to the 2.51 MeV level, which transition cannot be fitted with a DWBA analysis for $l = 2$ only. However, the derivation of the spectroscopic ratios of the odd and even parity member of the doublet is not reliable.

The angular distribution of the transition to the 3.738 MeV level is obscured by the $l = 0$ transition to the 0.871 MeV level of ^{17}O. Comparison with the angular distribution of the latter transition at an incident energy of 7.73 MeV [18]) indicates that an $l = 1$ component may not be present in the transition to the 3.738 MeV level of ^{24}Na.

Sperduto and Buechner [12]) have found two groups of levels in ^{24}Na, one consisting of levels at 3.850, 3,899 and 3.929 MeV and the other of levels at 4.184, 4.202 and 4.219 MeV. Although the resolution in their experiment is better than that of the present measurements, we propose levels at 3.88, 3.93 and 3.96 MeV in the first group and at 4.14, 4.16, 4.18 and 4.20 MeV in the second. In their spectra a fourth weak peak is present at the high energy side of the second group. This peak probably corresponds to the level at 4.14 MeV. In the present measurements the members of the groups are obtained from the change of the shape of the proton peak with angle. The relative position of these two groups to neighbouring peaks makes us confident to propose the new energy assignments. Jáidar *et al.* [19]) have published results of recent Q value measurements on ^{23}Na(d, p)^{24}Na at a deuteron energy of 1.81 MeV, in which they report for the Q value of the transition to the ground state 4.736 MeV instead of 4.731 MeV and in which they assign the following excitation energies of 0.472, 0.568, 1.347, 1.847, 1.893, 2.563, 3.754, 4.191 and 4.210 MeV to the levels at 0.472, 0.564, 1.341, 1.844, 1.884, 2.561, 3.738, 4.184 and 4.202 MeV (from MIT [12])), respectively. Both measurements agree within the experimental errors. However, the first authors might as well have identified the levels at 4.191 MeV and 4.210 MeV with those of MIT at 4.202 MeV and 4.219 MeV, within the experimental errors.

This assignment would support the above conclusion from the present work,

that the levels in this group have slightly lower excitation energies than the values given by MIT.

The level at 4.558 MeV has been found to be a doublet, one level at 4.53 MeV and one at 4.558 MeV.

Dalton, Parry and Scott [16]) have found levels at 4.41, 4.72, 4.91, 5.02, 5.13, 531 and 5.42 MeV, which, within the experimental accuracy of their and the present experiment, agree with the levels at 4.44, 4.75, 4.94, 5.04, 5.12, 5.33 and 5.40 MeV.

TABLE 5

Energies and intensities of γ lines in the $^{23}Na(n,\gamma)^{24}Na$ reaction

Groshev [22])		Kinsey [23])		Motz [24])		Burgov [25])		Motz [27])	Suggested transition	
E_γ	I	E_γ	I	E_γ	I	E_γ	I	E_γ	from level[a])	to level[a])
6.96	<0.1								6.96	0.000
								6.49	6.96	0.472
6.40	22	6.41	20			6.42	21	6.40	6.96	0.564
5.61	6	5.61	7.5			5.62	5.7	5.62	6.96	1.341
								5.44		
						(5.35)	(0.5)			
(5.12)	0.8	5.13	1.8					5.11	6.96	1.844
						(5.08)	(1.2)	5.07	6.96	1.884
(4.90)	1.2					(4.91)	(1.3)	4.90		
(4.70)	0.9					(4.72)	(1.3)	4.73	4.74	0.000
4.50	2.1					(4.54)	(1.3)	4.48		
								4.45	6.96	2.51
(4.30)	0.5					(4.29)	(0.7)			
4.18	2.1							4.18		
3.985	17.2	3.96	20			4.03	14.6	3.97	6.96	2.99
									4.44	0.472
3.86	5.9	3.85	11					3.88	4.44	0.564
(3.68)	1.3									
						3.64	13.2	3.64	(3.65	0.000)
3.617	18	3.60	10	3.59	18			3.58	6.96	3.37
3.56		3.56	20						6.96	3.409
								3.51		
						3.40	(2.3)	3.41		
								3.37	6.96	3.582
									3.37	0.000
3.30	5					(3.31)	(5)	3.28		
								3.21		
3.10	9.5			3.07	7	(3.11)	(8.2)	3.09	(5.66	2.561)
									(4.44	1.341)
									(3.648	0.564)
								3.02	3.582	0.564
								2.99	2.99	0.000
2.84	7							2.86	3.409	0.564
								2.81	6.96	4.16
									4.16	1.341

[a]) Excitation energies in MeV.

TABLE 5 (continued)

Groshev [22])		Braid [26])		Motz [24])		Burgov [25])		Motz [27])	Suggested transition	
E_γ	I	E_γ	I	E_γ	I	E_γ	I	E_γ	from level[a])	to level[a])
2.68	8.5									
2.52	21	2.53	19	2.51	15			2.51	6.96	4.44
									2.99	0.472
									2.51	0.000
2.41	10.5							2.42	2.99	0.564
						(2.36)	(13.5)	2.36		
2.21	7.5			2.21	8	(2.20)	(22.6)	2.22	6.69	4.75
									4.74	2.51
									3.582	1.341
								2.07	3.409	1.341
									(5.66	3.582)
2.020	11.5	2.02	12	2.03	13			2.03	(5.66	3.648)
									2.51	0.472
(1.95)	4							1.95	2.51	0.564
				1.90	3			1.90+		
(1.87)	5.5							(1.88?)	1.884	0.000
1.66	7.5	1.66	5	1.63	10			1.64	2.99	1.341
								1.57	3.409	1.844
1.35	6.5	1.35	6					1.37[b])	4.75	3.37
								(1.30?)+	(6.96	5.66)
								(1.28?)	1.844	0.564
0.875	44	0.86	34	0.877	30			0.86	3.37	2.51
									1.341	0.472
(0.790)	4.3							0.78	1.341	0.564
(0.710)	5								(2.561	1.844)
0.475	74	0.48	60	0.473	50				0.472	0.000
				0.090					0.564	0.472

[b]) Part of this γ line belongs to the transition ^{24}Mg (1.37) → ^{24}Mg (0.000), which line is in cascade with a γ line from ^{24}Mg (4.12) → ^{24}Mg (1.37) of 2.74 MeV. The difference in intensity between the two lines suggests, that part of the 1.37 MeV γ line is due to a transition between levels in ^{24}Na.

Actually the level at 4.75 MeV has been found first by El Bedewi and El Wahab [15]).

There is agreement in the l assignment to the transition to these levels; all levels have odd parity and are produced by transitions with probably both $l = 1$ and $l = 3$ components.

Other transitions with $l = 1$ and $l = 3$ components have been found at 4.62, 4.69, 4.97, 5.06, 5.18, 5.24 and 5.47 MeV. Transitions to levels at 5.57, 5.62, 5.66, 5.72, 5.76, 5.83, 5.89, 6.06, 6.17, 6.22, 6.28, 6.49, 6.55, 6.58, 6.69, 6.73, 6.81 and 6.88 MeV have been found. The analysis of the angular distributions to these levels is not possible, because the transitions to levels of ^{13}C, ^{14}C and ^{17}O obscure these angular distributions at too many angles. The transition to the 5.66 MeV level may have an $l = 0$ and $l = 2$ component. The lowest unbound state with spin 2^+ at 6.96 MeV, in which the neutrons of the (n, γ) reaction are captured, is obscured by the ^{1}H peak.

The level at 6.93 MeV with spin 2^+, proposed by Hibdon [20, 21]), to explain the width and the magnitude of the total cross section for neutron capture into the 6.96 MeV state, may either be obscured by the ^{1}H peak or it is identical to the level at 6.88 MeV. In that case, the transition to the 6.88 MeV level has probably $l = 0$ and $l = 2$ components, which is not evident from the obtained angular distribution.

8. Other Information about ^{24}Na

Information about other reactions and transitions has been collected in ref. [11]). Results of the ^{23}Na(n, γ)^{24}Na reaction [22–26]) are of particular interest in connection with the (d, p) data. Recent (n, γ) work has been done at Los Alamos [27]); however, no detailed information about the γ energies and the intensities of the γ lines is available. Table 5 represents a compilation of all information on the (n, γ) reaction. It also indicates to which transitions between levels of ^{24}Na these γ lines may correspond. These assignments differ slightly from those by Groshev *et al.* [22]) in the light of the fact that new levels have been identified in the present work.
An interpretation of the nuclear structure of ^{24}Na will be given in a second paper [28]) on the basis of the experimental data described in the present paper.

The author is grateful to Prof. W. C. Parkinson for making available to him the facilities of the Michigan cyclotron and for his stimulating support, to Dr. G. R. Satchler for the DWBA analysis of the angular distributions, and to Prof. K. T. Hecht and Prof. P. C. Gugelot for stimulating discussions. Prof. W. W. Meinke is thanked for suggesting the target thickness measurement by neutron activation analysis and Mr. H. M. Nass for performing the measurement. It is my duty to thank Prof. H. T. Motz for kindly making available to me the results of the ^{23}Na(n, γ)^{24}Na reaction prior to publication. The author wishes to acknowledge the contribution to this work by Mr. W. E. Downer and Mr. R. Pittman of the technical staff of the cyclotron and by Mrs. A. Klumpp, Mrs. B. Stark and Mrs. L. Graf of the plate scanning group. This work was supported in part by the US Atomic Energy Commission and by the Instituut voor Kernphysisch Onderzoek (I.K.O.), as part of the research program of the Stichting voor Fundamenteel Onderzoek der Materie (F.O.M.), which is supported by the Nederlandse Organisatie voor Zuiver Wetenschappelijk Onderzoek (Z.W.O.).

References

1) S. T. Butler, Proc. Roy. Soc. (London) **A208** (1951) 559
2) M. H. Macfarlane and J. B. French, Revs. Mod. Phys. **32** (1960) 567
3) R. H. Bassel, R. M. Drisko and G. R. Satchler, The distorted wave theory of direct nuclear reactions. I: "Zero range" formalism without spin-orbit coupling, and the code SALLY, ORNL-3240, UC-34-Physics (Oak Ridge National Laboratory, Jan. 26, 1962)
4) W. Tobocman, Theory of direct nuclear reactions (Rice Institute, August 1959)

5) D. R. Bach, W. J. Childs, R. W. Hockney, P. V. C. Hough and W. C. Parkinson, Rev. Scient. Instr. **27** (1956) 516
6) W. W. Meinke and R. W. Shideler, Nucleonics **20** (1962) 60
7) C. Daum, Thesis (University of Amsterdam, 1962)
8) C. Mayer-Böricke, R. Santo and U. Schmidt-Rohr, Nuclear Physics **33** (1962) 36
9) H. D. Scott, Nuclear Physics **27** (1961) 490
10) D. W. Miller, H. E. Wegner and W. S. Hall, Energy and orbital angular momentum dependence of Coulomb-distorted (d, p) angular distributions, unpublished report (Indiana University and Los Alamos Scientific Laboratory)
11) P. M. Endt and C. v. d. Leun, Nuclear Physics **34** (1962) 1
12) A. Sperduto and W. W. Buechner, Phys. Rev. **88** (1952) 574
13) R. Shapiro, Phys. Rev. **93** (1954) 290
14) W. F. Vogelsang and J. N. Mc Gruer, Phys. Rev. **109** (1958) 1663
15) F. A. El Bedewi and M. A. El Wahab, Nuclear Physics **21** (1960) 49
16) A. W. Dalton, G. R. Parry and H. D. Scott, unpublished report (University of Liverpool, Department of Physics)
17) D. Piraino, C. H. Paris and W. W. Buechner, Phys. Rev. **119** (1960) 732
18) E. J. Burge, H. B. Burrows, W. M. Gilson and J. Rotblat, Proc. Roy. Soc. (London) **A210** (1951) 534
19) A. Jáidar, G. Lopéz, M. Mazari and R. Dominguez. Rev. Mexicana de Fys. **10** (1961) 247
20) C. T. Hibdon, Phys. Rev. **118** (1960) 514
21) C. T. Hibdon, C. O. Muehlhause, W. Selove and O. Sala, Phys. Rev. **77** (1950) 730
22) L. V. Groshev, A. M. Demidov. V. N. Lutsenko and V. I. Pelekhov, Atlas of gamma-ray spectra from radiative capture of thermal neutrons (Pergamon, London, 1959)
23) B. B. Kinsey, G. A. Bartholomew and W. H. Walker, Phys. Rev. **83** (1951) 519
24) H. T. Motz, Phys. Rev. **104** (1956) 1353
25) N. A. Burgov and G. V. Danilyan, Izv. Akad. Nauk., Ser. Fiz. **20** (1956) 1941
26) T. H. Braid, Phys. Rev. **102** (1956) 1109
27) H. T. Motz, private communication, April 1961
28) C. Daum, Nuclear Physics, to be published